

# Surface and interface resonances in second harmonic generation from metallic quantum wells on Si(111)

K. Pedersen and T. G. Pedersen

*Department of Physics and Nanotechnology, Aalborg University, Pontoppidanstræde 103, 9220 Aalborg Øst, Denmark*

P. Morgen

*Fysisk Institut, SDU Odense, Campusvej 55, 5230 Odense M, Denmark*

(Received 19 May 2005; revised manuscript received 7 November 2005; published 29 March 2006)

The separation of surface and interface contributions to optical second harmonic generation from thin Ag and Au films on Si(111)  $7 \times 7$  forming quantum well levels has been investigated by spectroscopy over a broad frequency range. Resonances due to excitations of discrete quantum well levels have been investigated as a function of light frequency and film thickness. As a function of thickness the system goes through a series of resonances due to the shift of the levels with the width of the well. As a function of frequency these resonances shift toward lower thickness for increasing frequency. The frequency dependence also reveals the basic electronic resonances of the film and substrate materials existing independent of size quantization. In a mapping of resonances as a function of both thickness and frequency, avoided crossings are observed whenever quantum well resonances evolving with thickness coincide with basic electronic resonance frequencies. The dependence on thickness and frequency is well described by a model where the second harmonic signal originates from quantized levels at the two interfaces of the film and interferes with an interface contribution having the characteristic resonances of the Si interface layer. Using this description together with adsorption experiments it is demonstrated that the in-plane polarization is dominated by contributions from the buried interface while the polarization perpendicular to the surface contains contributions from both interfaces.

DOI: [10.1103/PhysRevB.73.125440](https://doi.org/10.1103/PhysRevB.73.125440)

PACS number(s): 78.66.-w, 68.35.-p, 73.20.-r

## I. INTRODUCTION

Optical second harmonic generation (SHG) from materials with bulk centrosymmetry such as metals and a number of elemental semiconductors, e.g., Si and Ge, is surface and interface sensitive due to the lack of electric dipole contributions to second-order nonlinearities in such materials.<sup>1</sup> Thin films on a substrate, having two dissimilar boundaries, are thus expected to be interesting objects for SHG studies. The buried interface can be reached even through metal films up to 50–100 atomic layers thick. However, the interface signal appears together with contributions from the rest of the system, in particular the free surface. Resonances that may appear in SHG spectroscopy can thus be localized either to the free surface or to the buried interface. Separation of different contributions thus requires modeling and experiments where the response of the free surface is modified.

A number of previous works have addressed resonant transitions at buried interfaces through SHG spectroscopy. Heinz *et al.*<sup>2</sup> investigated resonances at the Ca<sub>2</sub>/Si(111) using a combination of SHG and sum frequency generation. On Si/oxide interface systems resonances corresponding to critical points have been investigated intensively.<sup>3</sup> Also localized interface states with no relation to the bulk band structure have been reported.<sup>4,5</sup> In these systems, however, the oxide film and the free surface are not expected to contribute significantly to SHG and it is clear from the outset that the main contribution to the signal comes from the buried interface. Interface resonances are thus seen directly from the SHG spectra.

Here we focus on thin metallic films on semiconductors that under proper growth conditions form crystalline layers

with monatomic height variations within a probing area with millimeter dimensions. Parallel to the results presented here, quantum well (QW) effects have been investigated carefully using synchrotron radiation photoemission spectroscopy on samples prepared under identical deposition conditions. In combined photoemission and SHG experiments, a clear correspondence between the sharpness of QW peaks in valence band spectroscopy and oscillations in SHG as a function of film thickness<sup>6</sup> has been demonstrated. Several previous works have investigated SHG from various metal-metal<sup>7–9</sup> and metal-semiconductor<sup>6,10–12</sup> systems forming QW states. Kirilyuk *et al.*<sup>7</sup> developed a model describing periodic oscillations in SHG as a function of thickness on the basis of experiments on Au and Cu wedge-shaped films grown on Co(0001) substrates. From considerations based on the symmetry of simple QW levels they were able to explain the periodic variation in SHG with thickness. In a work by Luce *et al.*<sup>9</sup> microscopic calculations were used to analyze these oscillations and their dependence on photon energy and on the relative magnitude of surface and interface contributions.

In the present work the focus is on the interference between QW resonances and basic electronic resonances in film and substrate materials. By SHG spectroscopy covering the frequency range from below *d*-band transitions in the metal films to above the two lowest interband transitions at the substrate interface it is demonstrated that resonances at the buried interface can be identified through the dispersion of QW resonances seen with SHG. Compared to previously reported results the wide frequency range combined with modifications of the free surface by adsorption of foreign atoms and modeling of resonances in the system allow con-

siderable progress in the identification of various contributions to SH spectra from metal-semiconductor systems. We would like to point out the analogy to photoemission spectroscopy where several investigations over the last decade have shown that information about interfaces buried under metal films several tens of atomic layers thick can be revealed from QW effects in valence band spectra.<sup>13,14</sup> Though the electrons detected in the experiments originate only from the last few atomic layers at the free surface the energy levels of these electrons are determined by the quantization conditions perpendicular to the surface and thus the reflection coefficient (amplitude and phase) at the buried interface. The interface is thus probed by looking at the tail of a wave function that extends from the interface to the free surface. Interface information is typically deduced from the dispersion of QW levels with energy and with the wave vector component parallel to the surface. In SHG the corresponding plots show the photon energy of SH resonances versus film thickness. SHG resonances may be detected directly in intensity scans since the buried interface may be probed directly by the light. However, in a plot of SHG resonances versus film thickness phase changes accompanying interface resonances are revealed in dispersion curves due to interference of interface contributions with contributions from the rest of the system.

## II. EXPERIMENTAL RESULTS

The experiments were performed on samples mounted in a vacuum system equipped with low-energy electron diffraction (LEED) and a manipulator allowing liquid nitrogen cooling (to 170 K) and direct resistive heating of the samples. Sample cleanliness was verified by Auger electron spectroscopy in combination with LEED. The samples were cut from a 1-mm-thick *n*-type wafer with a resistivity of 5  $\Omega$  cm. Gold and silver films were deposited from an *e*-beam evaporator. A quartz crystal oscillator was used to calibrate the deposition rate. Wedge-shaped films were grown by moving the sample into the shade of a fixed screen during deposition. All details in sample cleaning and thin film deposition have been carefully investigated in parallel experiments at a synchrotron radiation photoemission facility.<sup>6</sup> The SHG experiments were performed with a femtosecond Ti:sapphire laser in the wavelength range from 700 to 1000 nm. A wider spectral range was obtained with an optical parametric oscillator (OPO) pumped by the third harmonic of 6 ns pulses from a *Q*-switched neodymium-doped yttrium aluminum garnet (Nd:YAG) laser. All experiments have been performed at 60° angle of incidence. The SH signals were detected by photomultiplier tubes after filtering out the fundamental light with colored glass filters.

Figure 1 shows scans of SHG versus film thickness recorded at room temperature from a Ag(111) wedge grown at 170 K with a clean Si(111)7 $\times$ 7 part in one end and 45 monolayers (ML) Ag at the other. After growth at low temperature the sample was allowed to anneal at room temperature for a few hours before SHG experiments. This procedure leads to growth of Ag domains with QW levels in photoemission and oscillations in SHG versus film thickness that are

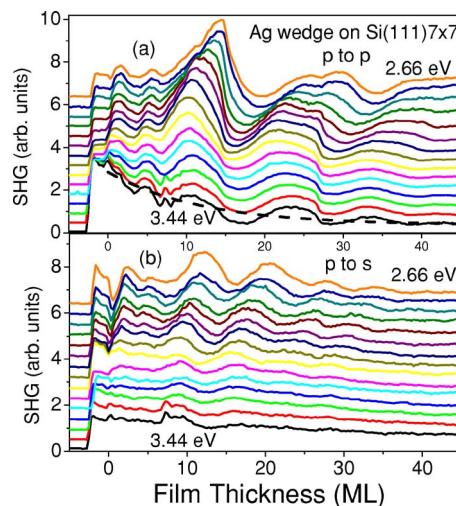


FIG. 1. (Color online) SHG as a function of Ag film thickness recorded for (a) *p*-polarized and (b) *s*-polarized SH fields at fundamental photon energies between 2.66 and 3.44 eV. The curves have been displaced vertically with the zero levels indicated at the start of the scans. The dashed curve on (a) shows the exponentially decaying background of the signal at 1.72 eV.

considerably sharper than those of films grown directly at room temperature.<sup>6</sup> The data have been recorded at 15 different SH photon energies in the range from 2.66 to 3.44 eV using femtosecond pulses from a Ti:sapphire laser. In order to separate the graphs they have been shifted vertically. The zero values can be read from the start of the curves. The curves have been scaled to the same average value in order to focus on the oscillatory behaviour of the signals. With the chosen azimuthal orientation of the sample the *p*-to-*p* polarization (field in plane of incidence) configuration used in Fig. 1(a) gives the isotropic contribution to SHG,<sup>15</sup> while the anisotropic part is isolated in the *p*-to-*s* (SH field perpendicular to incidence plane) configuration shown in Fig. 1(b).

Consider first the recordings of the isotropic signal in Fig. 1(a). Between the zero signal level outside the sample and the start of the Ag wedge (zero film thickness) a narrow region with a 7 $\times$ 7 reconstruction gives a signal that is relatively strongest at 3.44 eV due to the two-photon surface resonance, the  $E_0$ - $E_1$  transition, at the lowest direct interband transition energy. Following this, independent of photon energy, there is a fast rise in the signal during the first 2 ML, probably due to the formation of a Ag wetting layer. At higher coverage the signals show oscillatory behavior with a period that depends on photon energy. Starting with the lowest photon energy the peaks move toward lower coverage as the photon energy is increased. As the photon energy increases toward 3.0 eV the oscillation period becomes constant. At 3.44 eV the oscillations clearly appear on an exponentially decaying background. This background is caused by a two-photon  $E_0$ - $E_1$  resonance at the buried interface that is observed through the growing Ag film, but is gradually weakened due to absorption in the metal.

The anisotropic signal in Fig. 1(b) also shows an oscillatory variation with thickness that depends on photon energy in a similar way as the isotropic signal. However, the period tends to be shorter than for the isotropic part of the signal.

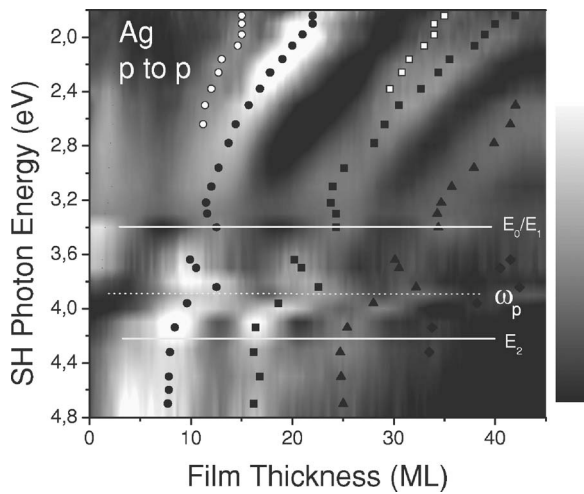


FIG. 2. Contour plot of *p*-polarized SHG from a Ag wedge based on scans of SHG as a function of film thickness recorded at 25 different photon energies. The plot is generated by interpolation of data between the 25 scans. The symbols mark the positions of signal maxima determined by inspection of the individual scans. The positions of Si critical points and the bulk plasma frequency of Ag are marked by horizontal lines.

The contrast in the variation, defined as the ratio between the oscillatory and the nonoscillating parts of the signal, is considerably less than for the isotropic part.

Thickness scans like those shown in Fig. 1 were recorded over a wider range of photon energies using the nanosecond OPO as pump source. Scans of the isotropic signal have been normalized to the same average level and then presented in Fig. 2 as contour plots with interpolation of data between the 25 scans. The symbols mark the positions of signal maxima determined by inspection of the individual scans. The representation with the photon energy of peaks increasing vertically downwards has been chosen in order to facilitate comparison to the standard representation of QW levels in valence band photoemission spectroscopy.<sup>13,14</sup> The dispersion of resonances toward lower film thickness for increasing photon energy seen at low energies clearly changes for SH photon energies near the bulk  $E_0$ - $E_1$  transitions. Data could not be recorded between 1.7 and 1.8 eV (3.4–3.6 eV SH energy) due to the degeneracy of the OPO. At the next bulk resonance  $E_2$  no clear change in the dispersion of resonances is seen. At low photon energies the resonance peaks split into double peaks [see also Fig. 1(a)]. The double peaks are only marked where they can be observed directly without mathematical treatment of the data.

A comparison of isotropic and anisotropic parts of the SHG signals is shown on Fig. 3 for 2.86 eV SH photon energy. It is noticed that the isotropic signal shows a very high contrast with almost vanishing signal at the minima in the oscillations while the contrast in the anisotropic part is much lower. A double-peak structure where the signal goes through two maxima in a single period is clearly seen in the isotropic part. The anisotropic part, on the other hand, tends to show more regular oscillations with half the period of the isotropic signal. The positions of resonances in the anisotropic part of the signal for a wider photon energy range are shown on the

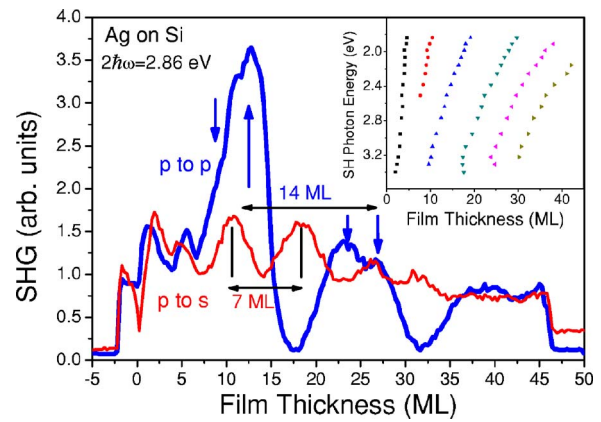


FIG. 3. (Color online) Comparison of the thickness oscillations of *p*- and *s*-polarized SHG from a Ag film. The period lengths of the oscillations are marked. The inset shows the positions of resonance peaks for *s*-polarized SHG in a thickness–photon energy plot.

inset of Fig. 3. In this case the resonances were very difficult to identify for SH photon energies above 3.4 eV as the curve at 3.44 eV in Fig. 1(b) already indicates. Thus, only resonances at low energies are included in Fig. 3. The dispersion of the resonances tends to change near the bulk  $E_0$ - $E_1$  resonance as for the isotropic part though the effect is not as pronounced.

Scans of SHG versus thickness have been recorded from a Au wedge grown on a  $\sqrt{3} \times \sqrt{3}$ -Au-reconstructed Si(111) surface. The Au-reconstructed surface was first formed by deposition of 5 ML Au on the  $7 \times 7$  surface followed by annealing to 1000 K. After that the Au wedge was grown. All depositions were done at room temperature. Previous investigations have shown that in terms of QW effects, the use of this Au-reconstructed surface as substrate leads to a better Au film than growth directly on the  $7 \times 7$  surface.<sup>11</sup> Figure 4 shows the positions of maxima in the thickness oscillations of the isotropic SH signal for different photon energies. The inset shows scans recorded with SH photon energies from 2.54 to 3.44 eV. The Au data show oscillations with a period

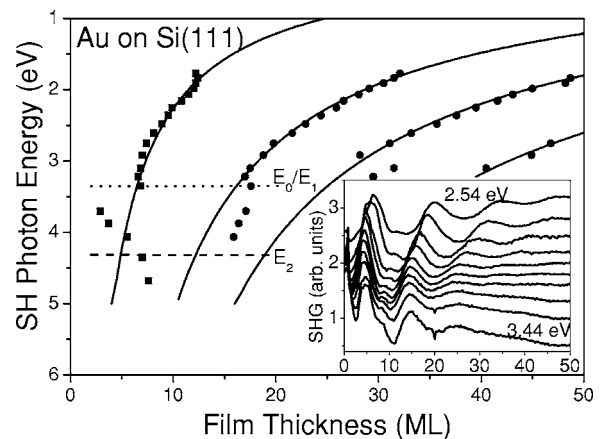


FIG. 4. Positions of resonance peaks in *p*-polarized SHG from a Au wedge on Si(111). The positions of Si critical points are marked by horizontal lines. The inset shows a number of thickness scans recorded with SH photon energies between 2.54 and 3.44 eV.

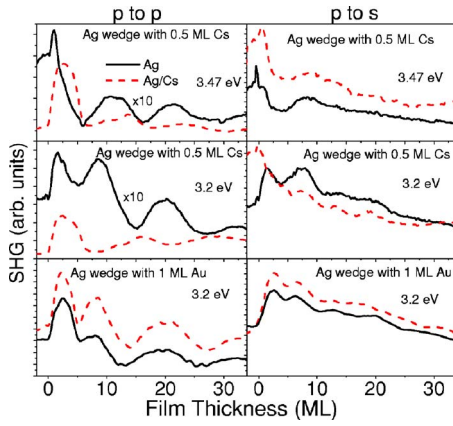


FIG. 5. (Color online) SHG as a function of thickness of a Ag wedge before and after deposition of (a)–(d) 0.5 ML Cs and (e) and (f) 1 ML Au. (a), (c), and (e) have been recorded with  $p$ -polarized SH light while (b), (d), and (f) have been recorded with  $s$ -polarized SH light.

that depends on pump photon energy in the same way as the corresponding data for Ag (Figs. 1 and 2). At low energies the positions of peaks move toward lower thickness as the photon energy increases. However, as also seen for the Ag film, the variation in peak positions change when the photon energy reaches the level where direct interband transitions in the Si interface layer become possible. The contrast in the oscillations gets weak as the photon energy increases due to effects of the Au  $d$  bands appearing about 2 eV below the Fermi level. Thickness oscillations for Au in SHG excited with pump photon energies from about 2 eV and up are thus much weaker than corresponding oscillations for Ag films where the  $d$  bands appear 4 eV below the Fermi level.

Contributions from both interfaces of the metal films are in general expected to contribute to the SHG signal. In order to distinguish between the two contributions it is useful to modify the free surface. It is difficult to get information by oxygen adsorption since very large exposures are needed before surface modifications are seen for noble metals. At such high exposures there may be effects of water adsorption that, at least for thin films, can affect the buried interface as well. Instead, submonolayer coverage of alkali metals can be used since this is known to dramatically change surface properties and thus also the nonlinear response of the free surface.<sup>16,17</sup> Figures 5(a)–5(d) compares thickness oscillations recorded along a Ag wedge before and after deposition of approximately half a monolayer of Cs. First it is noticed that the overall signal level for  $p$ -polarized SHG has increased by an order of magnitude after Cs deposition while the  $s$ -polarized signal has the same level. The LEED pattern of the surface is maintained after Cs deposition.

As another example of surface modification a single layer of Au was deposited on a Ag wedge. Figures 5(e) and 5(f) compare the SH signals as functions of the Ag wedge thickness before and after Au deposition. In this case there is very little effect of the overlayer regardless of polarization combinations and pump photon energy. This is in fact what one would expect since Au and Ag have the same lattice constant. Effects of the Au  $d$  bands do not seem to be important,

probably because of the low thickness of the Au layer.

### III. PHENOMENOLOGICAL MODEL

In this section we investigate a very simple model of SHG from a thin film forming QW's. The focus is on the peaks in SH as a function of film thickness and the way they shift with photon energy. It is assumed that the SH signal has contributions from the free surface and the buried interface of the metal film. These two contributions reflect the quantization of levels. In addition, resonances at critical points of the Si interface layer are introduced as a nonoscillating contribution. The nonlinear response of the surface and the interface of the metal film are described by second-order susceptibilities  $\chi_S$  and  $\chi_I$ , respectively, that vary periodically with film thickness with identical periods.

In order to describe this periodic variation the nonlinear susceptibility is represented by terms of the form

$$\chi_{S,I}^{(2)}(\omega) = \sum_{2,3} \frac{f_j^{S,I} Z_1 Z_2 Z_3}{(E_{21} - \omega)(E_{31} - 2\omega)} \quad (1)$$

where  $Z_i$  are transition matrix elements and  $E_{ij}$  are the energy differences between levels  $i$  and  $j$ . Assuming transitions between free-electron-like subbands in a QW of thickness  $d$  from the level with quantum number  $n$  to one numbered  $n + \Delta n$  leads to energy differences of the form

$$E_{ij} = \frac{\hbar^2 \pi^2}{2md^2} (2n\Delta n + \Delta n^2). \quad (2)$$

Assuming that the initial level is at the Fermi energy leads to  $n = k_F d / \pi$  where  $k_F$  is the Fermi wave vector. We will only consider films that are several monolayers thick. In that case  $n$  is much larger than  $\Delta n$  and the last term in (2) can be ignored. Clearly, Eq. (1) has a complicated frequency dependence with resonances at both  $\omega$  and  $2\omega$  as well as multiple (simultaneous) resonances. If the uppermost level is in the continuum at the substrate conduction band, however, resonances at the  $E_{21}$  transition will dominate the oscillating part of the SH signal. Thus, only the  $\omega$  resonance is considered in the following. With these assumptions the surface and interface susceptibilities in our phenomenological model can be represented by

$$\chi_{S,I}^{(2)}(\omega) = C \sum_{\Delta n} \frac{f_j^{S,I}}{\left( \frac{\hbar^2 k_F \pi}{md} \Delta n - \omega - i\gamma \right)} \quad (3)$$

where a broadening of the resonance has been introduced through the parameter  $\gamma$ . In (3) the dependence of the matrix elements on  $\Delta n$  has been ignored.

Oscillations in SHG with film thickness have previously been treated by Kirilyuk *et al.*<sup>7</sup> They observed that the oscillation period in SHG from Au on Co was twice the period found in linear measurements of the magneto-optical Kerr effect. This was explained by the higher sensitivity to symmetry of SHG compared to linear optics. Thus, since the QW levels giving resonances have approximately alternating odd and even characters a full period observed in SHG will in-

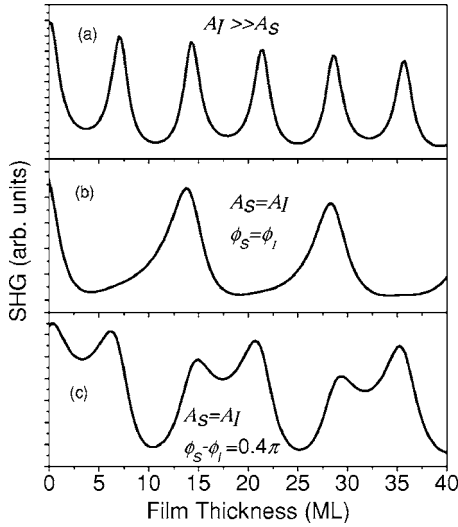


FIG. 6. SHG as a function of film thickness calculated from Eqs. (1)–(5) with (a) the interface contribution dominating the signal, (b) comparable surface and interface contributions, and (c) a phase difference between comparable surface and interface contributions.

clude resonances with one odd and one even wave function. Linear optics, on the other hand, does not depend on the symmetry of the wave function. In order to model this alternating odd and even character of the wave functions alternating signs of the susceptibilities in Eq. (3) are introduced through the factors  $f_j^{(S)}$  and  $f_j^{(I)}$  choosing  $f_j^{(S)} = 1$  and  $f_j^{(I)} = (-1)^{(j-1)}$ .

The SH field is given by the sum of the oscillating fields generated at the surface ( $E_S$ ) and at the interface ( $E_I$ ), and a nonoscillating background contribution ( $E_B$ ) where

$$E_S = A_S e^{i\phi_S} \chi_S, \quad (4)$$

$$E_I = A_I e^{i\phi_I} \chi_I e^{i2k_\omega d} e^{ik_2\omega d}, \quad (5)$$

$$E_B = \chi_B e^{i2k_\omega d} e^{ik_2\omega d}. \quad (6)$$

Here  $\phi_S$  and  $\phi_I$  describe the relative phase differences between the contributions and  $A_S$  and  $A_I$  are amplitudes of the surface and interface contributions relative to the background. The decay and phase change of pump and SH fields through the metal are described by the wave vectors  $k_\omega$  and  $k_{2\omega}$ . Figure 6 shows SH intensities calculated with this model for different values of  $A_S$ ,  $A_I$ , and the phase difference  $\phi_I - \phi_S$ . In Fig. 6(a) the magnitude of the interface susceptibility is much larger than that of the free surface. This leads to oscillations in SHG with a period  $p$  that is determined by the subband transitions at a single interface. The same situation would appear if the surface contribution were much larger than that of the interface. Another situation appears if the two susceptibilities (surface and interface) are of comparable magnitude as shown in Fig. 6(b). This leads to oscillations in SHG with a period that is twice that of the individual susceptibilities ( $2p$ ). As described in the work by Kirilyuk *et al.*<sup>7</sup> this is caused by the destructive interference by every second resonance due to the alternating odd-even symmetry

of the wave function. For symmetry reasons the susceptibilities of the two interfaces have opposite signs.<sup>7</sup> Thus, for SHG dominated by an even wave function the contributions from the two interfaces cancel while they add constructively for the asymmetric wave functions. Finally, in the case where the phase angle  $\phi$  differs from zero the signal shows alternating high and low peaks with an overall period equal to  $2p$  as shown in Fig. 6(c). Furthermore, the peaks appear in a double-peak structure with a pair of peaks close together followed by a larger low-signal part before the next pair of peaks appears.

With the model described for the SH intensity it is now possible to simulate data of the type shown in Fig. 2. It should be stressed that the goal is not to fit the model in details to the experimental data. This would not make sense since the model contains too many parameters. Furthermore, surface roughening on the atomic monolayer level leads to broadening of the SH resonances that, if it should be described, would add further parameters to the model. The goal here is rather to catch the main trends in the experimental data and thus use the model to identify the mechanisms behind the way the oscillations in SHG with thickness depend on photon energy.

In order to model the frequency dependence of the Si interface signal resonances with Lorentzian line shapes of the form

$$\chi_B^{(2)}(2\omega) = \sum_m \frac{f_m e^{i\phi_m}}{2\omega - \omega_m + i\gamma_m} \quad (7)$$

are introduced at the energy of the bulk  $E_0$ - $E_1$  transitions (3.37 eV) and at the  $E_2$  transition (4.3 eV). SHG from the surface of a bulk Ag(111) crystal around the bulk plasma frequency at 3.9 eV has been investigated by Li *et al.*<sup>18</sup> They found a resonance in the SH signal at the plasma frequency where strong interband transitions take place. By analyzing both the isotropic and the anisotropic contributions using the formalism of Sipe *et al.*,<sup>15</sup> they concluded that the signal variation with photon energy could be accounted for by the linear optical properties. It was thus not necessary to introduce effects of surface state transitions in the surface response tensor in order to describe the experimental results. Following these results the frequency dependence of the surface and interface contributions to SHG in the present work have been modeled by the expressions given by Sipe *et al.*<sup>15</sup> using the experimental linear optical properties of Ag from Palik.<sup>19</sup>

A contour plot of a simulation of the SH signal that should be compared to the experimental data in Fig. 2 is shown in Fig. 7. The simulation is based on a sum of the fields in Eqs. (4)–(6) with QW and interface resonances described by Eqs. (3) and (7), respectively. The parameters are relative amplitudes and phases of the resonances as well as their spectral positions. The oscillating character and general shift of the QW resonances toward lower thickness for growing photon energy is described by the model. By introducing an effective mass of 1.2 times the free electron mass the period of oscillations has been adjusted to the experimentally observed oscillations in Fig. 2. Resonances have been intro-

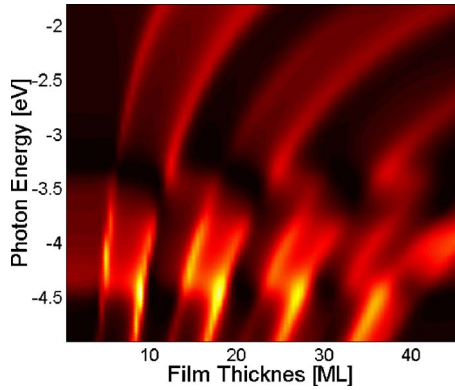


FIG. 7. (Color online) Simulation of the thickness and frequency dependence of SHG from Ag based on the model described in Sec. III. The calculated results should be compared to the experimental results in Fig. 2.

duced at 3.37 and 4.3 eV in the nonoscillating background signal from the Ag/Si interface. The positions of these resonances have been chosen at the bulk critical points. Though effects of the Ag/Si interface are expected this has not been clearly resolved in the experiments. In the simulations these two resonances have the same amplitudes. The frequency dependence of the oscillating QW contributions from the surface and the interface is determined by the linear properties of Ag with a plasma resonance at 3.9 eV as described above. Below the resonances the surface and interface contributions have comparable magnitudes (ratio 2.5 of interface to surface contribution) and  $\pi$  phase difference. This leads to the long oscillation period with a double-peak structure observed experimentally at low photon energies. In the region of the Si interface resonances and the plasma frequency of Ag the phase relations among the different contributions get more complicated, leading to nonmonotonic dispersion of QW resonances with photon energy. Some of the details in the behavior near resonances will be discussed below.

The simulations carried out here describe the isotropic part of SHG. In this phenomenological model, simulations of the anisotropic signal would be done by changing relative amplitudes and phases of the nonlinear susceptibilities. However, such simulations of anisotropic SHG corresponding to the experimental results on Fig. 3 are less informative than those of the isotropic part since the effect of QW resonances almost vanish in the region where they could interfere with the Si interface resonance. Modeling of the anisotropic signal is thus not taken any further here.

#### IV. DISCUSSION

The SHG scans from Ag and Au films show a number of similarities. For both materials SHG versus thickness oscillates with a period that decreases with increasing photon energy. In addition, plots of resonance energy as a function of film thickness reflect resonances at the buried interface. The oscillation period for  $p$ -polarized SHG at 2.8 eV SH photon energy is 13 ML for both materials. For Au this value is consistent with results of Kirilyuk *et al.*<sup>7</sup> Rather similar oscillation periods are expected for Au and Ag films since the

two monovalent metals have the same lattice constant. Also Al films on Si(111) show QW oscillations with a dispersion of resonances that changes near the  $E_0$ - $E_1$  transitions as previously demonstrated by the present authors.<sup>12</sup> In the case of the trivalent Al the oscillation period in  $p$ -polarized SHG is shorter than for Ag and Au, namely, 9 ML, at 2.8 eV SH photon energy. As for Ag and Au the period of QW oscillations for Al is doubled in  $p$ -polarized SHG compared to  $s$ -polarized light. The QW resonances investigated in detail here for Ag thus have a number of features that seem to be general for SHG from thin films on Si. In the following we first discuss surface and interface contributions to the SH signal and then the frequency-dependent QW resonances near the bulklike Si and Ag resonances.

Investigations of Ag film growth on Si(111)  $7 \times 7$  by scanning tunneling and atomic force microscopy have shown flat domains separated by areas covered by a very thin Ag wetting layer.<sup>20</sup> The importance of these regions with very little Ag can be addressed on the basis of the thickness dependence of the  $p$ -polarized SHG at 3.44 eV shown in Fig. 1(a). At this photon energy the Si surface is resonantly excited and resonant conditions are expected to persist at the Ag/Si interface as the Ag layer grows, leading to a high interface signal. The dotted curve on Fig. 1(a) is a fit to the data with a decay constant of 10 MLs. This is even faster than the 18 ML predicted from the bulk optical properties of Ag.<sup>19</sup> The difference can be due to a higher electron scattering rate caused by the interfaces of the film. The fast decay of the interface signal is taken as a sign of very little contribution to SHG from areas between the Ag domains. It thus makes sense to neglect the island structure in the analysis of the SHG results. The appearance of QW oscillations in SHG as well as the sharp QW peaks observed in valence band photoemission<sup>6</sup> is a strong indication of flat Ag domains with little height variation among the domains. This justifies the model used for analysis of the data where it is assumed that the film is smooth with two sharp interfaces.

The oscillations in SHG with thickness show an overall trend toward a shorter period for increasing photon energy. Luce *et al.*<sup>9</sup> have discussed the thickness oscillations and their dependence on photon energy. They consider (i) comparable interface contributions as opposed to dominance of one interface and (ii) the dominance of electronic excitations in a narrow range of  $k$  points in the Brillouin zone as opposed to excitations involving a larger  $k$  space volume. Electronic excitations in a narrow part of the Brillouin zone generally lead to sharp QW resonances and frequency dependence of the oscillation frequency. This situation was found for Cu thin films on Co by Volmer *et al.*<sup>8</sup> In the work by Kirilyuk *et al.*,<sup>7</sup> on the other hand, the SHG oscillations with thickness for Au on Co(0001) were found to have a very weak dependence on frequency. This was explained by electronic excitations above the  $d$ -band transition energy of 2.38 eV covering a wide range of  $k$  points.

The appearance of period doubling as a result of alternating destructive and constructive interference of surface and interface contributions of the same order of magnitude has already been discussed on the basis of the phenomenological model above. Kirilyuk *et al.*<sup>7</sup> found period doubling for Au on Co(0001) while in the case of Cu on Fe Vollmer<sup>8</sup> found

dominance of the interface and thus no interference that could cause period doubling. In the present work the isotropic contribution, for both Ag and Au films, tends to oscillate with a period that is twice as long as that of the corresponding anisotropic contributions. This indicates that the isotropic contribution is composed of comparable surface and interface contributions while the anisotropic part is dominated by a single interface.

In the present case of Ag and Au on Si the oscillation periods clearly depend on the light frequency, contrary to the case of Au on Co.<sup>7</sup> For the Ag film the SH photon energy is below the onset of *d*-band transitions in the range where the oscillation period depends on frequency. The excitations are thus dominated by the free-electron-like *sp* band where it is expected that a narrow range of *k* points contribute for a given light frequency. Excitations of such states have been described theoretically in a previous work by the present authors.<sup>21</sup> The difference between frequency dependencies for Au on Si and Au on Co (Ref. 7) indicates that the substrate plays an important role. Below the onset of *d*-band excitations at a photon energy of 2.4 eV excitations of the *sp* bands as in the case of Ag dominate and a similar dispersion is expected. However, as it is seen from Fig. 5 this dispersion of resonances continues to the onset of interband transitions at the Si interface. Thus, the oscillating part of the response is presumably dominated by *sp* bands even in cases with sufficient photon energy to excite *d* bands.

Further information about the relative magnitude of surface and interface contributions comes from the surface modifications by Cs and Au deposition. SHG has been shown to be highly sensitive to the presence of alkali metal atoms on the surface which may lead to strong enhancement of SHG.<sup>16,17</sup> In the present experiments deposition of half a monolayer of Cs on the surface leads to an order of magnitude increase in the SHG signal for the polarizability perpendicular to the surface. However, even though some of the contrast in the SHG oscillations is lost, the same oscillation period as before Cs deposition is easily recognized. Maxima and minima positions at 3.47 eV are unchanged by the Cs layer while minima and maxima are interchanged at lower photon energies. The quantum well nature of the electronic levels excited in the SHG process is thus maintained during the order-of-magnitude enhancement of the signal. The effect of Cs deposition can thus not be described simply as an additional contribution from the free surface. Rather, the Cs atoms enhance the amplitude of the oscillating SHG signal and change the phase of the surface contribution. It is suggested that this can be explained in terms of the strong dipole field at the surface created by the charge transfer from the alkali atoms to the Ag surface. The field shifts the bands of the Ag film as directly demonstrated in photoemission experiments by Neuhold and Horn.<sup>14</sup> If the result is just a shift of all QW levels it is clear that the QW oscillations in the SH signal are preserved after Cs deposition. However, the overall signal level, including the oscillating part, increases upon Cs adsorption. We suggest that one of the effects of the field from the Cs atoms is to reduce the symmetry of the wave functions of the QW and thus enhance SHG. Finally, from the phenomenological model it is easy to describe the interchange of maxima and minima in the oscillations by a 180°

phase shift of the surface contribution introduced by the Cs layer.

The discussion above of the modification of the surface by Cs adsorption shows that the isotropic SH signal has surface and interface contributions of comparable magnitudes. The behavior of the signal could not be described by a single surface contribution. The anisotropic contribution, on the other hand, shows much smaller effect of the Cs layer. This points to the interface contribution as the main source of the SH signal.

With the help of the simulations leading to Fig. 7 it is possible to investigate the different features of the data in Fig. 2 that deviate from the overall dispersion of resonances with photon energy. Consider first a case where a single source (surface, interface or bulk) gives the SHG signal. A resonance in optical excitations will only appear in the intensity of the signal (unless phase sensitive detection is used). Plots like those in Figs. 2 and 7 will thus not directly show any change in dispersion of QW resonances due to additional resonances caused by, e.g., plasmons. If, on the other hand, two or more contributions are present the phase change at a resonance in one contribution will appear through the interference with the other contributions. The interplay between destructive and constructive interference will therefore affect the position of peaks in SHG versus thickness.

For the isotropic contribution to SHG Fig. 2 clearly shows resonances at SH photon energies of 3.37 and 3.9 eV corresponding to the  $E_0-E_1$  Si critical point and the bulk plasmon energy of Ag, respectively. The shape of the QW resonance dispersion curves where they break up and show opposite dispersion at the two sides of the resonances is modeled by the phenomenological theory (Fig. 7). Consider first a fixed photon energy. The thicknesses where the resonance maxima are observed depend on the interference with the other contribution to the SH field. If the phase of this other contribution changes this will shift the thicknesses where the signal maxima are observed. Now, letting the photon energy change from one side to the other of a resonance leads to a  $\pi$  phase shift in this contribution, thus interchanging thicknesses with constructive and destructive interference. This leads to the sharp changes in QW dispersion curves at 3.4 and 3.9 eV. Thus, these breaks in QW dispersion curves appear when two types of resonances meet: the QW resonances evolving periodically with film thickness and the photon energy determined resonances at the Si interface or at the Ag plasma frequency.

## V. CONCLUSIONS

Thin films of Ag and Au grown on Si(111) surfaces show oscillations in SHG intensity as a function of film thickness that can be described as an effect of quantization of the electronic levels due to confinement in the direction perpendicular to the film. The isotropic SHG signal has comparable contributions from both interfaces over a wide range of photon energies. This appears from (i) the long period in oscillations of the signal with film thickness, (ii) the change in the signal level and its thickness dependence upon Cs adsorption, and (iii) the sensitivity of QW resonances to the pres-

ence of resonances at the Si-metal interface. The anisotropic signal, on the other hand, has a short oscillation period and shows little sensitivity to Cs adsorption as a result of the dominance of the buried interface.

The QW resonances in SHG have been investigated by mapping out their positions as functions of thickness and photon energy. They show an overall dispersion to lower thickness with increasing photon energy. Deviations from this monotonous dispersion appear at photon energies where the QW resonances interfere with contributions having resonances in bulklike electronic properties such as direct interband transitions in the Si interface layer and plasmons in Ag. The dependence of SHG on both photon energy and film thickness can be described by a model where the metal film

is represented by interfering contributions from the two interfaces, both of which pass through a series of resonances as the film thickness increases. In addition, the Si interface layer has a contribution with resonances at the critical points of the band structure of the interface layer. When resonances evolving in the thickness scale meet resonances evolving in the photon energy scale avoided crossing of resonance peaks are observed. This is explained by interference of two comparable contributions to SHG that shift from constructive to destructive when passing through a resonance. Representations of QW resonances in thickness-energy plots analogous to those used for valence band photoemission data are thus very useful in the identification of resonances in SHG from thin films.

- 
- <sup>1</sup>G. A. Reider and T. F. Heinz, in *Photonic Probes of Surfaces*, edited by P. Halevi (Elsevier, Amsterdam, 1995).
- <sup>2</sup>T. F. Heinz, F. J. Himpsel, E. Palange, and E. Burstein, *Phys. Rev. Lett.* **63**, 644 (1989).
- <sup>3</sup>W. Daum, H.-J. Krause, U. Reichel, and H. Ibach, *Phys. Rev. Lett.* **71**, 1234 (1993).
- <sup>4</sup>S. Bergfeld, B. Braunschweig, and W. Daum, *Phys. Rev. Lett.* **93**, 097402 (2004).
- <sup>5</sup>G. Erley, R. Butz, and W. Daum, *Phys. Rev. B* **59**, 2915 (1999).
- <sup>6</sup>K. Pedersen, T. B. Kristensen, T. G. Pedersen, P. Morgen, Z. Li, and S. V. Hoffmann, *Surf. Sci.* **482-485**, 735 (2001).
- <sup>7</sup>A. Kirilyuk, Th. Rasing, R. Megy, and P. Beauvillain, *Phys. Rev. Lett.* **77**, 4608 (1996).
- <sup>8</sup>R. Vollmer, in *Nonlinear Optics in Metals*, edited by K. H. Bennemann (Oxford Science Publications, Oxford, 1998).
- <sup>9</sup>T. A. Luce, W. Hübner, A. Kirilyuk, Th. Rasing, and K. H. Bennemann, *Phys. Rev. B* **57**, 7377 (1998).
- <sup>10</sup>T. G. Pedersen, K. Pedersen, and T. B. Kristensen, *Phys. Rev. B* **60**, R13997 (1999).
- <sup>11</sup>K. Pedersen, T. G. Pedersen, T. B. Kristensen, and P. Morgen, *Appl. Phys. B: Lasers Opt.* **68**, 637 (1999).
- <sup>12</sup>K. Pedersen, P. K. Kristensen, J. Rafaelsen, N. Skivesen, T. G. Pedersen, P. Morgen, Z. Li, and S. V. Hoffmann, *Thin Solid Films* **443**, 78 (2003).
- <sup>13</sup>T.-C. Chiang, *Surf. Sci. Rep.* **39**, 181 (2000).
- <sup>14</sup>G. Neuhold and K. Horn, *Phys. Rev. Lett.* **78**, 1327 (1997).
- <sup>15</sup>J. E. Sipe, D. J. Moss, and H. M. van Driel, *Phys. Rev. B* **35**, 1129 (1987).
- <sup>16</sup>S. Arekat, S. D. Kevan, and G. L. Richmond, *Europhys. Lett.* **22**, 377 (1993).
- <sup>17</sup>A. Liebsch, *Phys. Rev. B* **40**, 3421 (1989).
- <sup>18</sup>C. M. Li, L. E. Urbach, and H. L. Dai, *Phys. Rev. B* **49**, 2104 (1994).
- <sup>19</sup>*Handbook of Optical Properties of Solids*, edited by E. D. Palik (Academic, Orlando, FL, 1985).
- <sup>20</sup>G. Meyer and K. H. Rieder, *Surf. Sci.* **331-333**, 600 (1995).
- <sup>21</sup>T. G. Pedersen, K. Pedersen, and T. Brun Kristensen, *Phys. Rev. B* **61**, 10255 (2000).